Mixed magnetic phases in tetragonal $TbRu_2Si_2$

1998 J. Phys.: Condens. Matter 10 3919

(http://iopscience.iop.org/0953-8984/10/17/020)

J. Phys.: Condens. Matter **10** (1998) 3919–3927. Printed in the UK PII: S0953-8984(98)88888-7

Mixed magnetic phases in tetragonal $TbRu_2Si_2$

A Garnier†, D Gignoux†§, D Schmitt† and T Shigeoka‡

† Laboratoire de Magnétisme L Néel, CNRS, BP 166, 38042 Grenoble Cédex 9, France
‡ Faculty of Science, Yamaguchi University, Yamaguchi 753, Japan

Received 31 October 1997

Abstract. A careful analysis of neutron diffraction experiments under magnetic field performed on a single crystal of tetragonal $TbRu_2Si_2$ is presented. It shows that the zero-field–low-temperature magnetic phase is not the *natural compensated antiphase* structure proposed so far for the $Q = (3/13, 0, 0)$ propagation vector, but a *mixed* phase where the moment of two of the 26 Tb sites of the unit cell vanishes. The magnetic structures of the first three field induced phases of the multistep metamagnetic process agree with previous analysis whereas the fourth field induced phase is not the non-mixed proposed one but a mixed one with two zero moments as in zero field. Contrary to previous interpretations, the transition at 4.7 K observed by specific heat and susceptibility corresponds to the change of the magnetic structure from the mixed low-temperature one to a slightly modulated non-mixed one. Numerical simulation allowed us to account for the main properties observed and emphasizes the crucial role of the crystal field.

1. Introduction

$TbRu_2Si_2$ belongs to the large series of rare earth R based compounds having the tetragonal $ThCr_2Si_2$-type structure (space group $I4/mmm$) and which present a great variety of magnetic properties (Gignoux and Schmitt 1997). In particular, due to the frustration of RKKY-type exchange interactions and the large uniaxial anisotropy, the field–temperature magnetic phase diagrams are often complex. This is the case for $TbRu_2Si_2$ on which the following properties have been established. (i) It orders at $T_N = 56$ K into an incommensurate amplitude-modulated structure of propagation vector $\boldsymbol{Q} = (\tau, 0, 0)$ with $\tau = 0.23$ in reduced units, magnetic moments being along the $\boldsymbol{c}$ axis due the strong magnetocrystalline anisotropy (Slaski *et al* 1984). (ii) At low temperature a squaring up of the modulation develops and a structure with equal moments was announced to occur at 3.1 K (Chevalier *et al* 1985). (iii) Just above $T_t = 4.7$ K a two-step metamagnetic process is observed along $\boldsymbol{c}$ (figure 1), the intermediate phase being a double-$\boldsymbol{Q}$ structure (Shigeoka *et al* 1992, Kawano *et al* 1993). (iv) Below T_t, the metamagnetic process along $\boldsymbol{c}$ is much more complex (figures 1 and 2). It exhibits at least six sharp transitions, the steps of the five first transitions being close to $M_s/26$, where $M_s = 9\ \mu_B$ is the saturation magnetization per Tb atom (Shigeoka *et al* 1995b, Garnier *et al* 1995). As neutron diffraction experiments on a single crystal showed that the high-temperature propagation vector persists below T_t in zero field and up to the sixth transition it has been considered that $\boldsymbol{Q}$ is commensurate with $\tau = 3/13 = 0.23$ (Shigeoka *et al* 1995a). The following interpretation of the intensities has

§ Corresponding author: Damien Gignoux, Laboratoire de Magnétisme L Néel—CNRS, BP 166, 38042 Grenoble Cédex 9, France. E-mail address: gignoux@grmag.polycnrs-gre.fr

0953-8984/98/173919+09$19.50

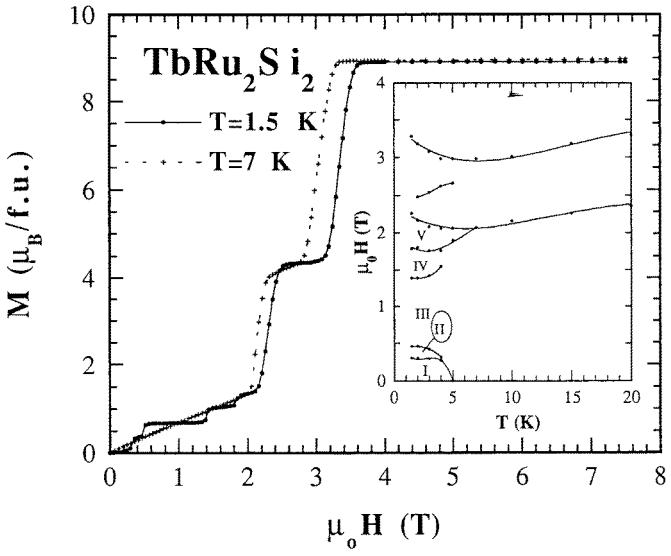

Figure 1. Magnetization processes along the ***c*** axis at 1.5 and 7 K. The inset shows the low-temperature region of the field–temperature phase diagram.

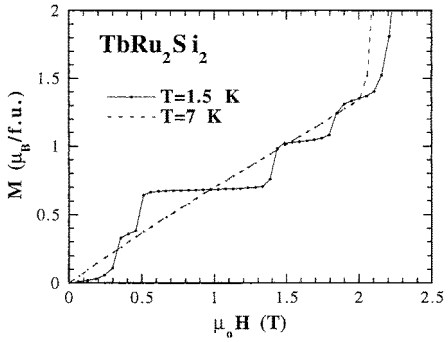

Figure 2. Details of the low-field magnetization processes at 1.5 and 7 K.

been given: in zero field the 26 magnetic moments of the unit cell have the *natural* antiphase structure ($5\bar{4}4\bar{5}4\bar{4}$) sequence, where '5' or '$\bar{4}$' means 5 or 4 successive ferromagnetic planes along the [100] direction with their moment along ***c*** up or down, respectively. The proposed first induced phase is a *mixed structure* with a sequence of the type ($5\bar{4}40\bar{4}4\bar{4}$) for instance, where '0' stands for one site with zero moment among the 26 ones of the magnetic cell. This structure is in agreement with the observed step of $M_s/26$ whereas the flipping of the moments of one plane would lead to a step of $2M_s/26$. The magnetic field then induces a succession of *non-mixed* and *mixed* magnetic phases. (v) At T_t one observes pronounced anomalies of the susceptibility (Garnier *et al* 1995) and of the specific heat (Salgueiro da Silva *et al* 1995). The latter has been interpreted as a λ-type order–disorder transition of 1/13 of the magnetic moments, the zero-field magnetic structure above T_t being mixed with one over thirteen paramagnetic planes (Salgueiro da Silva *et al* 1995).

In order to check all these results and explanations, and to have a better insight into the magnetic properties of this compound, we reanalysed the neutron diffraction data on a single crystal and we did numerical simulations using the periodic field model.

2. Experimental results

Experiments were performed on a double-axis neutron diffractometer at the Research Reactor Institute, Kyoto University, Osaka. The incident wavelength was 1.006 Å. $\boldsymbol{q}$-scans of the type $(1k0)$ performed below T_t for $\mu_0 H = 0$, 0.35, 1.1, 1.6 and 1.9 T, i.e. in zero field (phase I) and within the first four field induced phases (phases II, III, IV and V), are shown in figure 3. For all these patterns, well defined peaks associated with fundamental

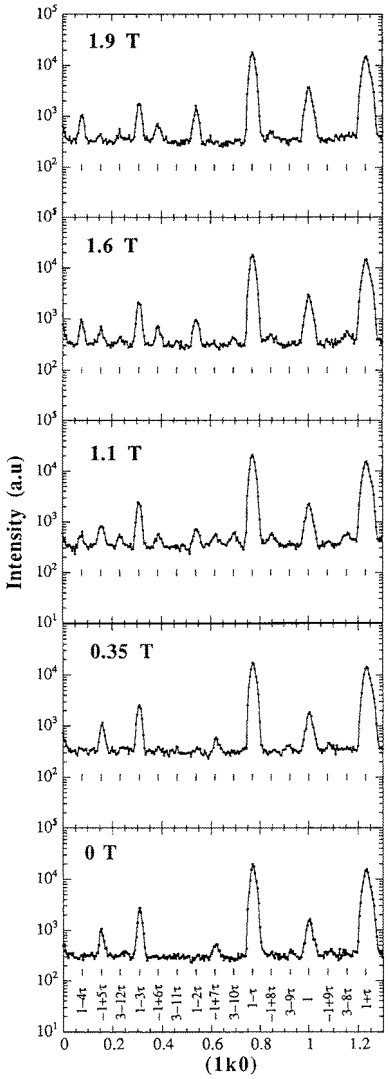

Figure 3. $\boldsymbol{q}$ scans of the type $(1k0)$ at 2.2 K in different applied fields. The values of k of the peaks corresponding to the $n\tau$ harmonics ($n = 1$ to 12) are reported in the lower part.

and higher-order harmonics of the same propagation vector were observed and allowed its accurate determination: $\tau = 0.230 \pm 0.001$ which confirms the lock-in of the periodicity on the commensurate value 3/13. With such a value of τ, keeping in mind that the structure is body centred, there are 26 independent sites in the magnetic cell and the magnetic moment can be described by means of 14 independent Fourier components:

$$\boldsymbol{M}(\boldsymbol{R}_i) = \sum_{n=-12}^{13} \boldsymbol{M}_{n\boldsymbol{Q}} \exp(\mathrm{i}n\boldsymbol{Q}\cdot\boldsymbol{R}_i) \qquad \text{with } \boldsymbol{M}_{-n\boldsymbol{Q}} = \boldsymbol{M}^*_{n\boldsymbol{Q}}. \tag{1}$$

The intensities associated with the components for $n = 1$ to 12 are well observed. For each field the modulus $|\boldsymbol{M}_{n\boldsymbol{Q}}|$ of these Fourier components have been deduced from the intensities after correction of the Lorentz factor and of the Tb form factor. The corresponding observed values of the $|\boldsymbol{M}_{n\boldsymbol{Q}}|/|\boldsymbol{M}_{\boldsymbol{Q}}|$ ratios are plotted versus the harmonic number in figure 4 (open squares and full lines). We did not determine the $n = 13$ Fourier component as the corresponding peaks fall on forbidden nuclear peaks of the type (hkl) with $h + k + l = 2n + 1$ where a small contribution of the $\lambda/2$ wavelength clearly appears on the spectrum in the saturated ferromagnetic induced phase. From the neutron diffraction patterns we did not extract the $n = 0$ Fourier component, associated with the ferromagnetic component, as the corresponding peaks fall on the nuclear peaks leading then to large uncertainties on its determination. We rather extracted this component with a good accuracy from magnetization measurements. For each pattern we have compared the $|\boldsymbol{M}_{n\boldsymbol{Q}}|/|\boldsymbol{M}_{\boldsymbol{Q}}|$ observed ratios with those calculated for all the possible structures compatible with the observed magnetization. In each case a unique structure accounts for the experimental values. The observed ratios are compared with those of the good model in figure 4(a) to 4(e). We also report in these figures the ratios of one or two tested models which do not account for the experiments. The magnetic structures of phase I to V are schematized in figure 5.

Surprisingly, the zero-field magnetic structure is not the natural previously proposed antiphase structure (Shigeoka *et al* 1995a) but a mixed structure with two Tb sites with zero moment per unit cell. Indeed the reliability factors

$$R = \sum_{n=1}^{12} ||\boldsymbol{M}_{n\boldsymbol{Q}}(\mathrm{obs})| - |\boldsymbol{M}_{n\boldsymbol{Q}}(\mathrm{cal})|| \Big/ \sum_{n=1}^{12} |\boldsymbol{M}_{n\boldsymbol{Q}}(\mathrm{cal})|$$

are 3.8% and 16.7% for the mixed and non-mixed phase, respectively. (The misinterpretation of the neutron diffraction data has been probably due to the fact that only the *natural* antiphase structure was considered to exist). Also the structure under 1.9 T is not antiphase ($R = 22.4\%$) but mixed with two zero moments ($R = 9.1\%$). The first and second transitions then involve sites with a $0 \rightarrow M_s$ process leading to a mixed phase with one Tb site with zero moment and then to a non-mixed phase, respectively. The third and fourth transitions involve $-M_s \rightarrow 0$ processes leading to new mixed phases with one and two Tb sites with zero moment, respectively.

In zero field there is no dramatic change of the neutron diffraction pattern when increasing temperature just above T_t. One mainly observes a slight reduction of the $n = 7$ and $n = 9$ harmonics which probably originates from a slight modulation of the moment amplitude near the node of the modulation due to thermal effects. Assuming constant or zero moments the experimental Fourier components slightly better fit with a non-mixed structure than with the low-temperature mixed one. This existence of a non-mixed phase just above T_t and in zero field is supported by the fact that there is no boundary between this region of the phase diagram and that corresponding to phase III (see inset

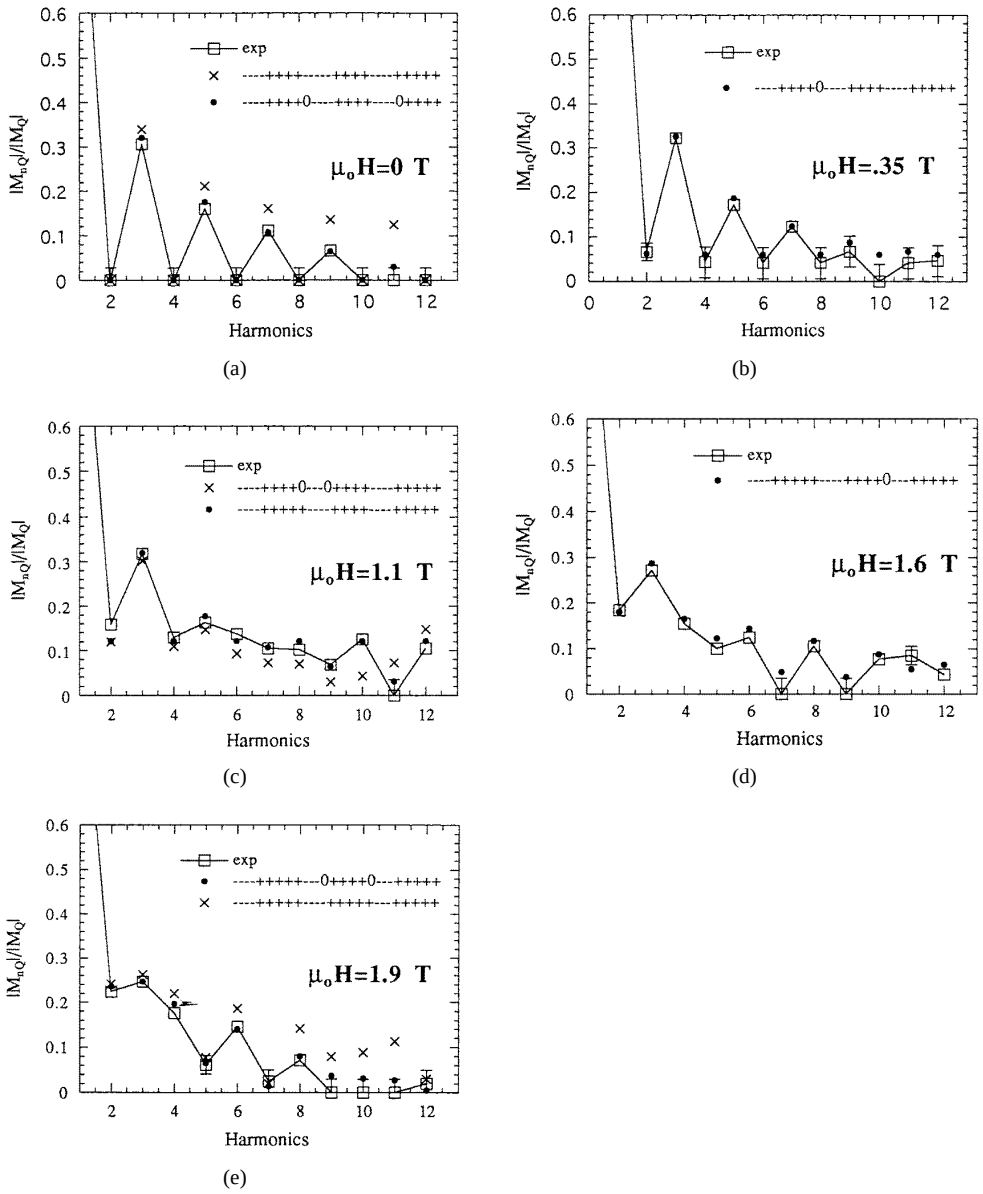

Figure 4. Experimental and calculated Fourier components of the magnetization, normalized to M_Q, at 2.2 K and under different applied fields. Squares are the experimental points. Black dots are the calculated points for the models which fit with the experiments. The reliability factor $R = \sum_{n=1}^{12} ||M_{nQ}(\text{obs})| - |M_{nQ}(\text{cal})|| / \sum_{n=1}^{12} |M_{nQ}(\text{cal})|$ is 3.8%, 9.3%, 6.4%, 10.0% and 9.1% for $\mu_0 H = 0$, 0.35, 1.1, 1.6 and 1.9 T, respectively. Other symbols corresponds to examples of some of the tested structures which do not agree with the experiments.

of figure 1). It can then be concluded that, at T_t, there is a transition from the low-temperature mixed phase toward a non-mixed phase associated with a shift of the phase of the modulation.

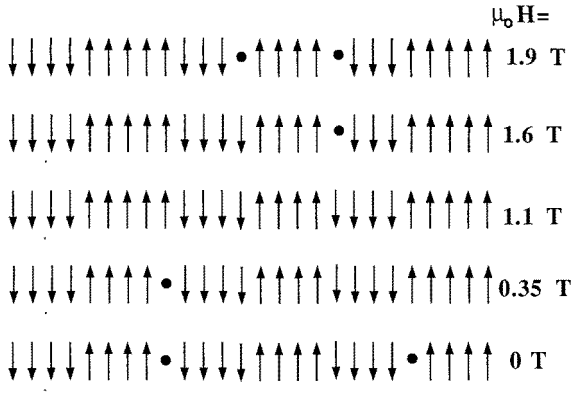

Figure 5. Schematic representation of the different magnetic structures. The sequence of the 26 Tb ferromagnetic plane along the propagation vector is shown.

3. Analysis and discussion

The results obtained from the joint analysis of magnetization and neutron diffraction experiments are quite original, in particular in zero magnetic field where a non-mixed structure was expected whereas a mixed one with two Tb atoms with zero moments per unit magnetic cell is observed. This result rejects the interpretation of the specific anomaly observed at T_t (Salgueiro da Silva *et al* 1995). Indeed this interpretation was based on the assumption of an antiphase structure at low temperature and a mixed phase above T_t whereas the contrary is observed.

Mixed magnetic phases have already been observed at low temperature in systems where magnetic interactions are frustrated when the magnetic element is close to a magnetic–non-magnetic (M–NM) instability. This latter situation is that found in the RMn_2 (R = rare earth) compounds where the 3d Mn magnetic moment is close to the Stoner criterion for the onset of itinerant magnetism (Ballou *et al* 1991) and in CeSb (Rossat-Mignod *et al* 1985, Kasuya *et al* 1993) or UNi_4B (Lacroix *et al* 1996) where the magnetic instability comes from the Kondo effect. In the compound under investigation with normal non-Kramers ions the only source of M–NM instability can be the crystalline electric field (CEF), the effect of which can lead to a non-magnetic singlet ground state.

In order to understand the origin of mixed phases in this type of uniaxial rare earth compound we have performed numerical simulations considering only the exchange and CEF interactions, the latter interaction being the same for all atoms as they belong to a unique crystallographic site whereas the exchange field can vary from one atom to the other. The approach was made in the frame of the self-consistent periodic field (PF) model which has already been used to describe quite satisfactorily the magnetic properties of rare earth antiferromagnets showing metamagnetic processes (Blanco *et al* 1992, Ball *et al* 1993). This PF model is based on an N-site Hamiltonian, N being the number of magnetic ions over one period, i.e. 26 in the present case:

$$\mathcal{H} = \sum_{i=1}^{N} \mathcal{H}_{CEF}(i) + \sum_{i=1}^{N} \mathcal{H}_z(i) + \sum_{i=1}^{N} \mathcal{H}_B(i). \tag{2}$$

The first term is the CEF coupling. The second term is the Zeeman coupling $-\mu_0 \boldsymbol{H} \cdot \boldsymbol{M}(i)$ between the internal magnetic field (external field corrected for demagnetizing field effect)

and the 4f moment at site i, $M(i) = -g_J\mu_B \boldsymbol{J}(i)$. The third term is the exchange interaction $-\mu_0 \boldsymbol{H}_{ex}(i) \cdot \boldsymbol{M}(i)$ where the exchange field can be written, in the mean-field approximation, as

$$\boldsymbol{H}_{ex}(i) = (g_J\mu_B)^{-2} \sum_{j\neq i} J(ij)\langle \boldsymbol{M}(j)\rangle = (g_J\mu_B)^{-2} \sum_n \sum_{j\neq i} J(ij) M_{nQ}\, \mathrm{e}^{\mathrm{i}n\boldsymbol{Q}\cdot\boldsymbol{R}_j}$$
$$= (g_J\mu_B)^{-2} \sum_n J(n\boldsymbol{Q}) \boldsymbol{M}_{nQ}\, \mathrm{e}^{\mathrm{i}n\boldsymbol{Q}\cdot\boldsymbol{R}_j} = \sum_n \boldsymbol{H}_{nQ}\, \mathrm{e}^{\mathrm{i}n\boldsymbol{Q}\cdot\boldsymbol{R}_j} \qquad (3)$$

where $\boldsymbol{M}_{nQ}$ and $\boldsymbol{H}_{nQ}$ are the components of the Fourier expansion of the magnetic moment and of the exchange field, which have then the same periodicity. $J(\boldsymbol{q})$ is the Fourier transform of the exchange interaction. The full Hamiltonian is diagonalized self-consistently for the N ions of the magnetic period, the M_{nQ} obtained after diagonalization being reinjected into the initial Hamiltonian through (3). For a set of CEF and $J(n\boldsymbol{Q})$ parameters, it is then possible to evaluate for any field and temperature, the magnetic moment on each site and the free energy. In our case the number of CEF parameters is five whereas in principle 14 $J(nQ)$ values are needed. Due to this large number of parameters it is a great task to determine them. Many data obtained from different types of experiment (inelastic neutron scattering experiment for instance) are required and, in their absence, we tried to find representative parameters with the purpose to show that mixed phases can be stabilized at 0 K.

The first step was to find CEF parameters in order to have a system with two Tb magnetic states: (i) one with a zero (or weak) moment below a threeshold field and (ii) the other with a high moment above this field. This arises when the ground state is a singlet and when the first excited level has a large intrinsic magnetic moment. Moreover the components of these levels are such that the effective field acting on the Tb ions must lead to a *crossing* between the two lowest levels (Ball *et al* 1992). A set of parameters was found which gives the calculated variation of the Tb moment as a function of the effective field reported in figure 6. Among these parameters, reported in the caption of this figure, the second-order one is close to the value which can be deduced directly from the shift at 300 K between the reciprocal paramagnetic susceptibilities measured along and perpendicular to the fourfold axis (Garnier *et al* 1995). Concerning the exchange interactions, the basic properties are accounted for with only two parameters, namely $J(0) = -30$ K and $J(\boldsymbol{Q}) = 35$ K. However in order to have calculated results closer to the experimental behaviour we have included two additional parameters, $J(2\boldsymbol{Q}) = 10$ K and $J(3\boldsymbol{Q}) = 8$ K.

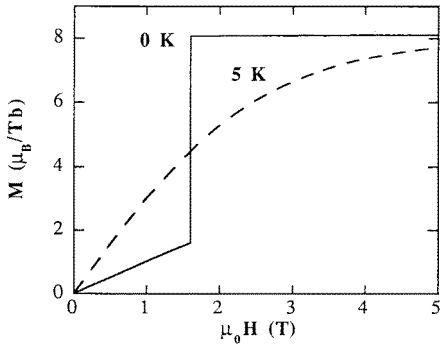

Figure 6. Calculated terbium moment, at $T = 0$ and 5 K, as a function of the effective field for the following CEF parameters: $B_2^0 = -8.0$ K, $B_4^0 = 5.3 \times 10^{-2}$ K, $B_4^4 = 2.0 \times 10^{-1}$ K, $B_6^0 = -5.8 \times 10^{-4}$ K and $B = 5.5 \times 10^{-3}$ K.

The main characteristics of the simulation are the following.

(i) At low temperature, in particular at 0 K, one obtained the metamagnetic process reported in figure 7 together with the field dependence of the energy of each phase. Phases I, II, IV and V are mixed phases identical to those observed. Phase III is the mixed phase ($\bar{4}40\bar{3}04\bar{4}5$) with two Tb atoms per unit cell with zero moment whereas the non-mixed phase ($\bar{4}5\bar{4}4\bar{4}5$) is observed. Note that the energy of the latter, the field dependence of which is reported in the dashed line in figure 7, is slightly higher than that of the former. In agreement with experiments, the amplitude of the steps is equal to $M_s/26$. It is worth noting that no mixed phase can be obtained if the ground state of the Tb ion is a magnetic doublet.

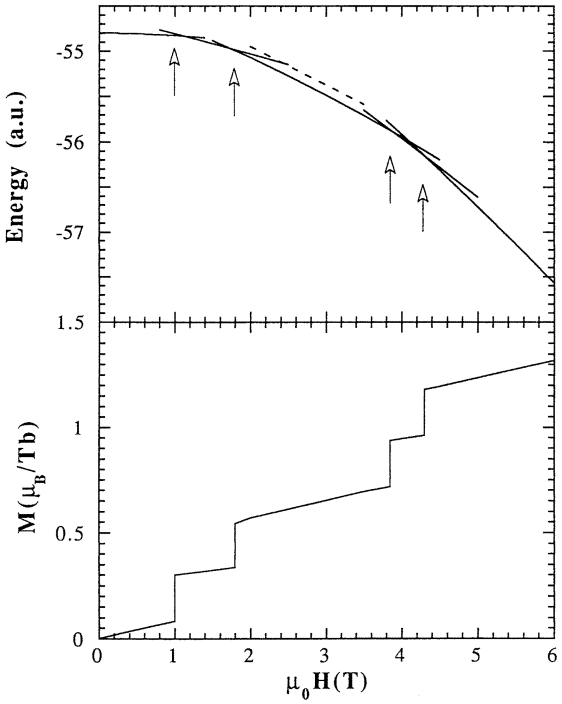

Figure 7. Numerical simulation at 0 K using the PF model. Lower part, low-field magnetization process in increasing field. Except the second field induced phase (III), all the other simulated phases (I, II, IV and V) are identical to the experimental ones. Upper part, field dependence of the energy of the different phases. Dashed line corresponds to the energy of the experimental non-mixed second field induced phase (III).

(ii) As observed, there are two transition temperatures: T_N at 58 K and a transition temperature T_t at 3.3 K. The latter corresponds to the transition from the low-temperature mixed phase toward the natural antiphase structure, slightly modulated. Although smaller than observed there is an entropy discontinuity at T_t. It is worth noting that, in zero field, the nature of the low-temperature mixed phase found in this study and that of the high-temperature phase previously assumed (Salgueiro da Silva *et al* 1995) to account for the specific heat measurements are quite different. In the present study there is no entropy associated with the sites with zero moment whereas in the previous interpretation a finite entropy ($R \ln 2$) is associated with these sites on account of the degeneracy of the magnetic ground state ($|\pm 6\rangle$).

(iii) The slope of M against H within each phase is twice as large for the mixed phase with two sites over 26 with zero moments as for a mixed phase with only one site with zero moment. Moreover this slope should be almost zero for a non-mixed phase as observed for phase III. This can be understood from the intrinsic initial susceptibility of M against H at 0 K shown in figure 6 and considering that there is no, one and two Tb atoms with zero moment over 26 for the non-mixed, mixed with one null moment and mixed with two null moments phases, respectively. These characteristics are effectively those observed, in particular for phases III, IV and V. On a more general point of view, this feature could be a good way to deduce in other materials, from the experimental variation of M against H and in the absence of neutron diffraction experiments, the nature of each phase, i.e. mixed or not mixed and, if mixed, the number of atoms with zero moment.

Acknowledgments

We warmly thank Professor N Iwata and Dr S Kawano for their contribution to the neutron diffraction experiments.

References

Ball A R, Gignoux D, Kayzel F E, Schmitt D and de Visser A 1992 *J. Magn. Magn. Mater.* **110** 337–42
Ball A R, Gignoux D, Schmitt D and Zhang F Y 1993 *Phys. Rev.* B **47** 11 887–96
Ballou R, Lacroix C and Nunez-Regueiro M D 1991 *Phys. Rev. Lett.* **66** 1910–3
Blanco J A, Gignoux D and Schmitt D 1992 *Phys. Rev.* B **45** 2529–32
Chevalier B, Etourneau J, Hagenmuller P, Quezel S and Rossat-Mignod J 1985 *J. Less-Common Met.* **111** 161–9
Garnier A, Gignoux D, Schmitt D and Shigeoka T 1995 *Physica* B **212** 343–50
Gignoux D and Schmitt D 1997 *Handbook of Magnetic Materials* vol 10, ed K H J Buschow (Amsterdam: Elsevier) pp 239–413
Kasuya T, Yanase A and Okuda K 1993 *Physica* B **186–188** 9–15
Kawano S, Shigeoka T, Iwata N, Mitani S and Ridwan 1993 *J. Alloys Compounds* **193** 303–5
Lacroix C, Canals B and Nunez-Regueiro M D 1996 *Phys. Rev. Lett.* **77** 5126–9
Rossat-Mignod J, Effantin J M, Burlet P, Chattopadhyay T, Regnault L P, Bartholin H, Vettier C, Vogt O, Ravot C and Achart J C 1985 *J. Magn. Magn. Mater.* **52** 111–21
Salgueiro da Silva M A, Sousa J B, Chevalier B, Etourneau J, Gmelin E and Schnelle W 1995 *Phys. Rev.* B **52** 12 849–51
Shigeoka T, Eguchi M, Kawano S and Iwata N 1995a *Physica* B **213/214** 315–7
Shigeoka T, Iwata N, Garnier A, Gignoux D, Schmitt D and Zhang F Y 1995b *J. Magn. Magn. Mater.* **140–144** 901–2
Shigeoka T, Kawano S, Iwata N and Fujii H 1992 *Physica* B **180/181** 82–4
Slaski M, Szytula A, Lecielewicz J and Zygmunt A 1984 *J. Magn. Magn. Mater.* **46** 114–22